Monitoring Mining Induced Plant Alteration and Change Detection in a German Coal Mining Area using Airborne Hyperspectral Imagery

Andreas Brunn[1]
Wolfgang Busch[1], Christoph Dittmann[2]
Christian Fischer[1], Peter Vosen[2]

INTRODUCTION:

Mining leads to inevitable changes in the environment, and that's why every European Mining company faces increasing environmental pressure and regulatory controls. Therefore a sound management of mining activities is of high concern to preserve nature and minimise the environmental impacts. Furthermore understanding and monitoring the environmental impact processes in mining areas is crucial for a sustainable management of Earth´s environment.

The investigations described here were carried out in the framework of the EU project MINEO on the Test Site Kirchheller Heide in Germany. MINEO is a shared cost project financed by the European Commission and each project partner. The project partners are 7 Geological Surveys from all over Europe and the Deutsche Steinkohle AG (DSK) as an industrial partner.

The Central European Test Site is located in western Germany in the north of the Ruhr District, one of the most congested industrialized regions with about 7.5 million inhabitants. About 40% of the test site area is covered with forests of different types and 50 % is used as farm land. The remaining 10 % are settlements and infrastructural installations. Because of its rural character the Test Site serves as a recreation area for the inhabitants of the Ruhr District. On the other hand DSK exploits hard coal from below this area from depths up to 1000 m applying longwall underground mining techniques. These mining activities lead to cavities in the rock which are not backfilled due to economic reasons. The collapses of these cavities are reproduced at the surface and subsidence movements occur. The procedure of these subsidence movements is described in the figure on the left. This phenomenon leads to specific environmental problems especially related to the water balance and to specific hydrological parameters. At the surface water logging zones can occur. Changes of the hydrological conditions in this small parcelled test area can lead to influences and changes of the ecological situation.

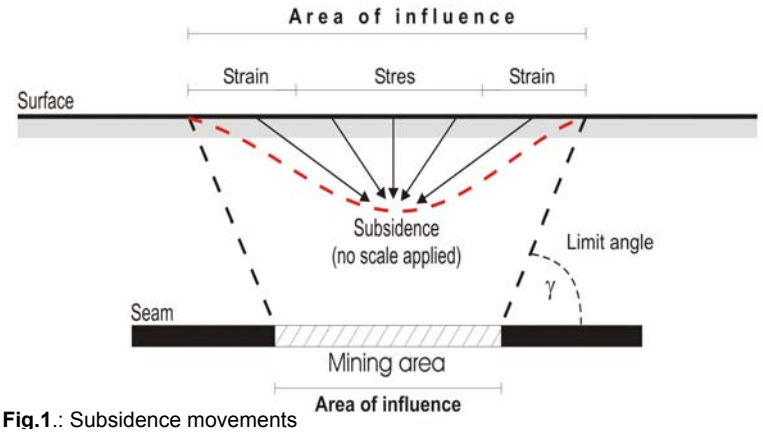

Fig.1.: Subsidence movements

[1] Technical University of Clausthal, Institute for Geotechnical Engineering and Mine Surveying, Erzstrass 18, 38678 Clausthal – Zellerfeld, Andreas.Brunn@tu-clausthal.de
[2] Deutsche Steinkohle AG, Division for Engineering Survey & Geoinformation Services, Karlstrasse 37 – 39, 45661 Recklinghausen, Christoph.Dittmann@deutsche-steinkohle.de

DATA PREPROCESSING

Airborne image data acquisition in contrast to spaceborne data recording is characterised by a comparatively low system stability. This results in geometric distortions due to variations in flight path and attitude of the plane. The distortions cannot be corrected satisfactorily with the traditional georeferencing procedures, since the plane movements, given by roll, pitch, yaw and heading angels, cannot be described by polynomial transformations of the image. A parametric approach is the preferable solution for the geocoding of high resolution airborne remote sensing data. This approach recalculates the flight scan geometry pixelwise applying auxiliary data measured physically. The three major types of auxiliary data are: image/scanner general information, navigation data (IMU and GPS) and a digital elevation model (DEM) for the equalisation. For our data we used the software package ParGe, especially designed for the geometric correction of airborne scanner data. ParGe theoretically gives the opportunity to georegister the data in subpixel-accuracy, but is highly dependent on the quality of the IMU data, the GPS-Track, the accuracy of the ground control points (GCP´s) and the used DEM.

The geocoding procedure was performed separately for each image strip. Theoretically only one GCP for each image strip is sufficient to estimate the roll/pitch or x/y values, in practice one GCP per 100 image lines was necessary to achieve a sufficient accuracy. The RMS error for the distortion after the geocoding has been calculated to 1,5-2 pixel (7 – 10 m) varying between the strips.

Fig.2: Example of a geocoded HyMap image combined with GIS vector data sets

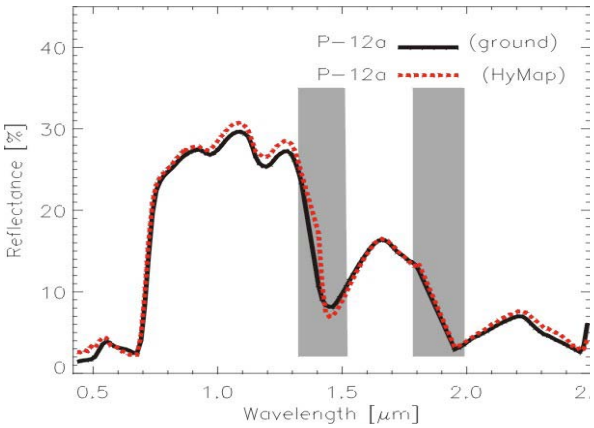

Fig.3: Comparison of ground-reflectance for a vegetation spectrum and the corresponding HyMap reflectance spectrum. The shaded vertical bars mark regions of strong atmospheric water vapour and CO_2 absorption.

For atmospheric correction several different approaches are in common use. For our tasks we used a physical model which is implemented in the Software ATCOR-4 applying the radiative transfer code MODTRAN, a further description of the method and the proceeding for our test site can be found in BRUNN ET.AL. 2001.

The accuracy of the atmospheric correction method described here depends on the factors calibration accuracy of the sensor, accuracy of the radiative transfer code and the quality of the image ortho-rectification. The deviation of ground measured reflectance and retrieved HyMap reflectance does not exceed 3%.

PLANT STRESS ESTIMATION

Vegetation spectra usually appear similar because the main reflectance components are the same. This fact requires the adoption of a different strategy to classify and to describe plants than the direct spectral feature and band shape matching used for geology applications. The spectral shape of plant leaves is controlled by absorption features of specific molecules and the cellular structure (ref. Fig. 4). Foliar absorption is primarily caused by photosynthetic pigments in the visible spectrum (VIS) (400-700 nm). The main pigments controlling the absorption are chlorophyll *a* and *b* and β-carotene. The amount of absorbed radiation depends on the pigment concentration. With increasing concentration, the green peak (around 550 nm) rises and the reflectance in the red range (670 nm) decreases.

For the estimation of plant stress three methods were adopted. These are the calculation and comparison of the red edge wavelength, the derivation of reflection features and the derivative analysis of vegetation spectra.

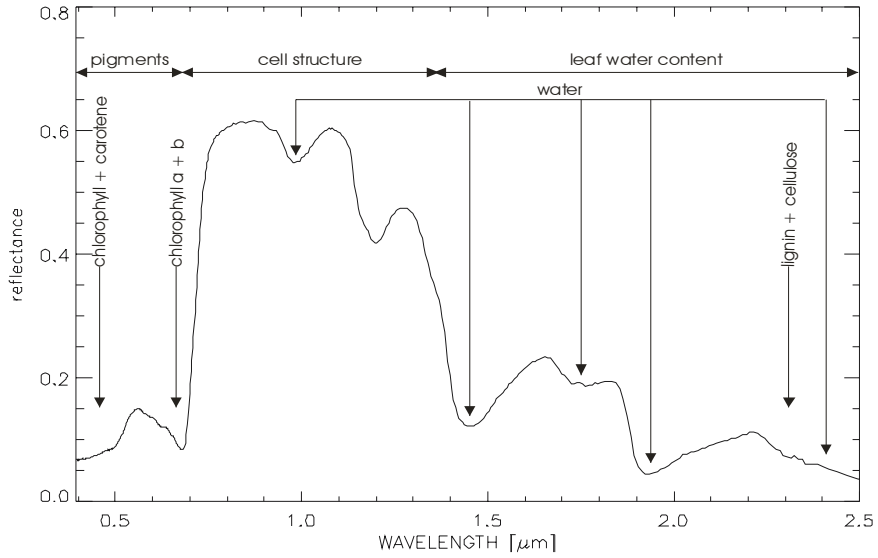

Fig.4: reflectance spectrum

Fig.4. shows a typical reflectance spectrum for vegetation between 0.42 and 2.48 µm. Between 0.68 and 0.8 µm, in the near infrared region, the spectrum rises steeply. This steep region is the edge of vegetation reflectance, where the chlorophyll pigment loses its ability to absorb energy. SINGHROY ET AL. (1991) found out, that stress induced shifts in the *red edge* may occur in both directions, towards the longer and shorter wavelengths. The *red edge* wavelength is defined as the position of the reflectance curve, where the second derivative of the strong increase between red and infrared wavelength equals zero.

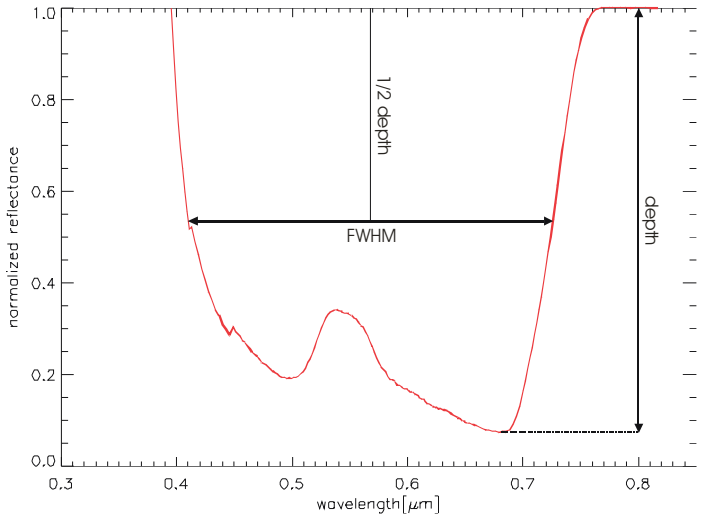

Fig.5: Continuum-removed example of a chlorophyll absorption in vegetation , (RENCZ, 1999)

The model implemented for this work uses a combined method of interpolation and linearization. First we interpolate the run of the curve with cubic spline functions. These functions can be derived twice to calculate the inflection point of

the reflectance curve. Because the algorithm for spline interpolations only delivers accurate derivative values of all measured points (but not for interstices between these points) it is only possible to calculate the two ambient points. After that we interpolate linearly between these two points and calculate the zero-point of the 2nd derivative from this linear interpolation, which represents the *red edge* wavelength. An important advantage using this spline interpolation is that splines directly touch every base of the spectrum that should be interpolated and influence the whole run of the interpolated curve. This characteristic of spline interpolations makes it possible to consider even subtle differences in the run of the reflectance curve.

The derivation of reflectance features using continuum removed spectra are based on the changes at the green reflectance peak near 0,57 µm, the chlorophyll absorption maximum near 0,68 µm and in the region of the infrared reflectance shoulder between 0,75 µm and 1.1 µm (SINGHROY ET AL, 1991). Absorption features, which commonly occur superimposed on a background slope in the source spectrum, are transformed into features with a uniform, flat background of 1.0 in the continuum removed spectrum. This allows each absorption feature in a spectrum to be mathematically analysed with respect to a consistent reference plane. The spectral features derived from this method are the maximum absorption depth (MaxAb), the full width at half maximum (FWHM) and a symmetry factor calculated by adding the logarithms of the absorption values on the left and the right side of the absorption maximum. Figure 5 gives a visualization of these three features.

The derivative Analysis originally developed for spectrometry (TALSKY, 1994) is the third method for the stress estimation and it is particularly promising for the use with hyperspectral remote sensing data. Derivatives not only emphasise subtle spectral details as well as changes but also suppress the mean level. Because of the noise sensitivity of this method a median filter with the window size of 5 was applied before we derived a spline function of the spectral curve and integrated the derivatives to calculate the areas (Fig.6).

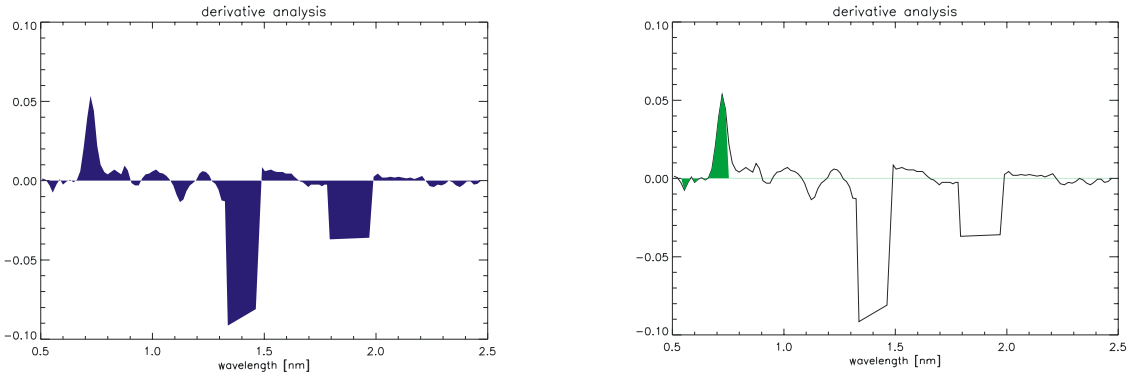

Fig. 6*:* Area of the first derivative over the whole spectral range (left) and area of the first derivative in the wavelength range between 0.54 and 0.78 µm, which is an interesting range for plant analysis (right).

One of the main subjects of the investigations on the Central European test site was the detection of vegetation stress caused by changes in the ground-water balance. As described above plant stress is spectrally expressed in a change of shape and wavelength of the vegetation edge at the transition between red and infrared wavelength. This shape was dressed in eighteen features. These features are Full width at Half maximum (FWHM), maximum absorption depth (MaxAb), Symmetry, *Red edge* Wavelength (*red edge*), minimum in red, Wavelength of the minimum in red, reflection maximum near 0.8 µ, wavelength region between the minimum in red and the *red edge* wavelength, area of the 1st. – 5th. derivative between 0.55 and 0.74 µm and the area of the 1st. – 5th. derivative between 0.42 and 2.5 µm.

Because changes of the plant status is expressed in the value of a difference from a standard value but not in the direction of this difference the following procedure for the stress detection have been applied on different forest stands: First a standard value for each feature and each forest class with no influence of the mining caused subsidence movements was determined using predefined endmember spectra.

a.) b.) c.)

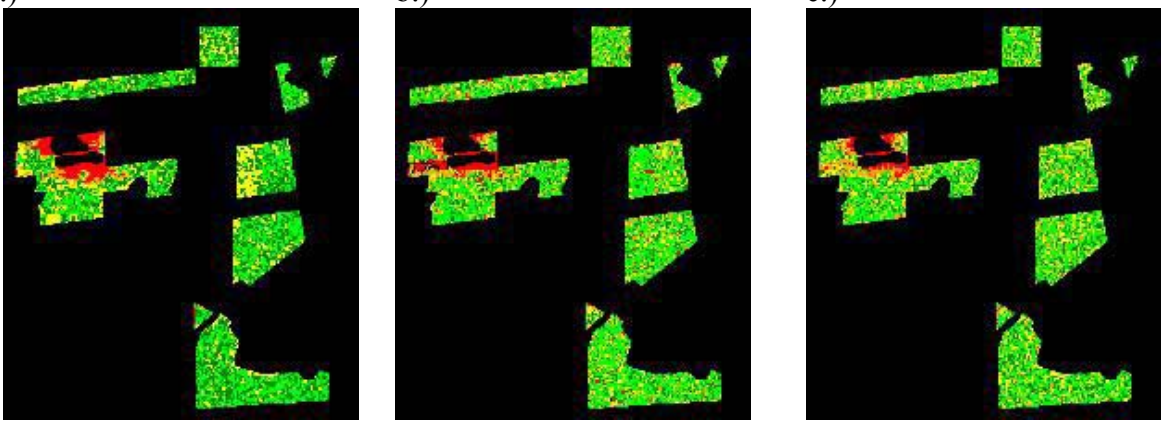

Fig. 7: Examples of plant stress mapping results using different promising features (description see text)

After that all the mentioned features for the hyperspectral image dataset were calculated. The stress evaluation took place by calculating the deviation from the standard feature values for each forest class separately, and the stress factor was defined as the absolute value of this deviation. For visualisation the last step was a threshold classification. Figure 7 shows the results of this stress detection algorithm for pine trees with the most promising features, the maximum absorption depth (a), the *red edge* wavelength (b) and the area below the second derivative in the wavelength region between 0.55 and 0.74 µnm (c).

CHANGE DETECTION METHOD

For the detection of land-cover status changes the 18 features implemented for stress detection were calculated for on the data of two temporally successive flight campaigns. Afterwards an absolute difference between the features calculated from data flown in 1998 and flown in 2000 was calculated. At last a change factor was defined as the absolute value of each particular feature. The figure below shows a scaled image of this change factor for the area of the second derivative between 0.55 – 0.74 µm.

Fig. 8 (left) shows increasing status changes from blue to red colors. It can be seen that many red colours are agricultural fields, which were planted in 1998 and was fallow in 2000 or vice versa. Strong changes are to be found on roads and houses, two. The reason for that can be found in the misregistration by 1-2 pixels of the two images. The detected changes on forest areas are real changes of plant health. Fig. 8. (right). shows real changes (increasing from green to red) of perennial plants (here pine trees). One can see that the most significant changes (red and orange colors) are concentrated round a lake which came up in the last years as a result of subsidence movements.

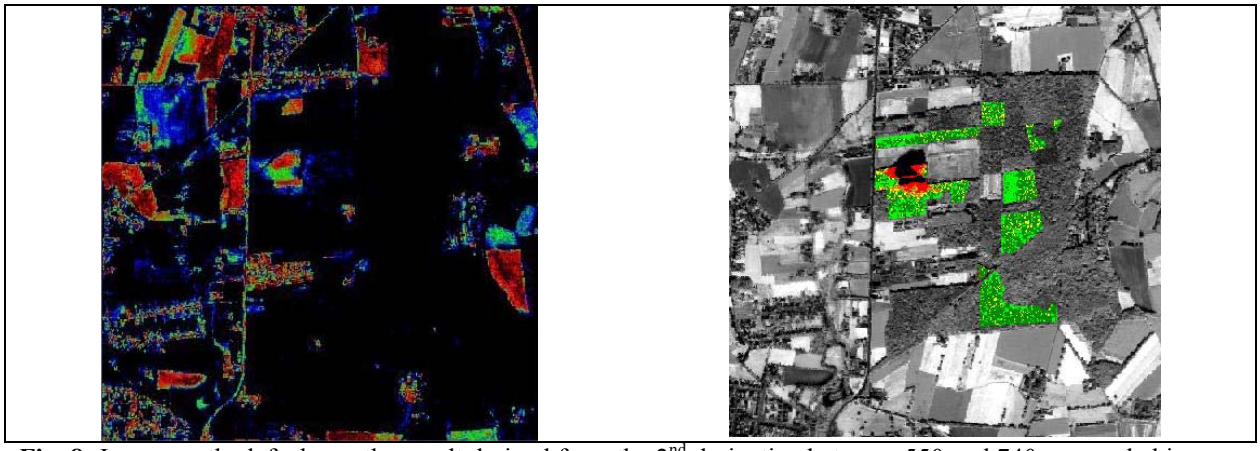

Fig. 8: Image on the left shows the result derived from the 2nd derivative between 550 and 740 nm, scaled image using a change factor, increasing plant stress from blue to red; the right image shows the same result for pine trees scaled and overlaid on a panchromatic HyMap channel, increasing stress from green to red.

Selected References

BACH, H.: Die Bestimmung hydrologischer und landwirtschaftlicher Oberflächenparameter aus hyperspektralen Fernerkundungsdaten, Münchener Geographische Abhandlungen, Reihe B, Band 21, 1995.

BRUNN, A., DITTMANN, C., FISCHER, C., RICHTER, R. :Atmospheric Correction of 2000 HyMap Data in the Framework of the EU-Project Mineo, Proceedings of the SPIE Workshop, Toulouse, September, 2001.

SINGHROY, V., KRUSE, F.: Detection of metal stress in Boreal Forest Species using the 0.67 µm chlorophyll absorption band; in: Proc. 8th. Thematic conference on geologic remote sensing, exploration, engineering and environment, Denver, 29. April – 2. May 1991, pp.361 - 372

TALSKY, G., Derivative Spectrophotometry, Weinheim, 1994